International Journal of Fatigue 41 (2012) 95–100

Contents lists available at SciVerse ScienceDirect

International Journal of Fatigue

journal homepage: www.elsevier.com/locate/ijfatigue

Growth of short cracks during low and high cycle fatigue in a duplex stainless steel

I. Alvarez-Armas [a,*], U. Krupp [b], M. Balbi [a], S. Hereñú [a], M.C. Marinelli [a,b], H. Knobbe [c]

[a] Instituto de Física Rosario – Consejo Nacional de Investigaciones Científicas y Técnicas (CONICET), Universidad Nacional de Rosario, Argentina
[b] Faculty of Engineering and Computer Science, University of Applied Sciences Osnabrück, Germany
[c] Institut für Werkstofftechnik, Universität Siegen, Germany

ARTICLE INFO

Article history:
Received 30 April 2011
Received in revised form 17 November 2011
Accepted 6 January 2012
Available online 24 January 2012

Keywords:
LCF
Duplex stainless steels
Embrittlement
Microstructure
Microcrack nucleation and propagation

ABSTRACT

Damage evolution during low- and high-cycle fatigue in an embrittled duplex stainless steel is characterized in this paper. Moreover, scanning electron microscopy observations (SEM) in combination with electron backscattered diffraction (EBSD) measurements and transmission electron microscopy (TEM) were employed in order to analyze microcracks formation and propagation. During low-cycle fatigue, microcracks initiate the ferrite phase either along slip planes with the highest Schmid factor (SF) inside the grains or at the α/α grain boundary. Then, microcracks propagation take place in ferrite or austenite grains with the highest SF. An analysis of the dislocation structure in the near-surface and in ferritic grains in the bulk of the specimen has shown that dislocation microbands are associated with microcrack initiation.

In the high-cycle fatigue regime, damage generally initiates in the austenite by slip band formation followed by crack initiation either at an α–α boundary or at an α–γ boundary in the intersection of slip bands in the austenite. The microstructure in the austenite consists of a low density of dislocation pile-ups while the ferrite is practically inactive or develops only micro-yielding at boundaries.

Despite the differences in both fatigue regimes, phase boundaries are an effective barrier against crack propagation because they delay the advance of the crack tip.

1. Introduction

Nowadays, duplex stainless steel (DSS) grades are used by a wide range of industries because of their excellent combination of mechanical properties and corrosion resistance. In many applications, they are subjected to cyclic loading and thus, the improvement of the prediction of fatigue life at different strain amplitudes seems to be necessary. To make such predictions, the identification of the mechanisms of damage on the microstructural scale is imperative in order to know when the microstructure provides an effective barrier against dislocation motion. In other words, to know when the onset of the fatigue crack propagation will occur. For this purpose, much work has been done on surface damage for different strain amplitudes [1–6]. This analysis is even more complex when one of the phases is embrittled by thermal heat treatment [7–11]. Aging duplex steels at 475 °C leads to the spinodal decomposition of the ferritic phase, which consists of α (Fe-rich) and α' (Cr-rich) phases that develop an internal stress field responsible for strengthening of the alloy. The plasticity of spinodal decomposed ferrite is reduced because of a reduction in the number of slip systems. Deformation by twinning may also take place in addition to deformation by dislocation glide [12,13].

This paper focuses on the identification of activated slip systems during low and high cycle fatigue in an aged duplex stainless steel. From scanning electron microscopy observations (SEM) in combination with electron backscattered diffraction (EBSD) measurements, the slip systems and their associated Schmid factor (SF) are analyzed in both constitutive phases and correlated to the microcrack path. Moreover, the dislocation structure developed mainly in the α/γ interphase was analyzed and correlated with the formation and propagation of microcracks.

2. Experimental procedure

The behavior of microstructurally short fatigue cracks was studied in the regime of low and high cycle fatigue in the duplex stainless steel, German standard DIN 1.4462. The chemical composition of the material in weight percent is: C: 0.02; Cr: 21.0; Ni: 5.6; Mo: 3.1; Mn: 1.8; N: 0.19; P: 0.023; S: 0.002; Fe: balance.

In order to increase the grain size, the steel was homogenized for 4 h at 1250 °C; slow cooled to 1050 °C and finally water quenched. The microstructure consists of a balanced proportion of austenite in ferrite with a mean grain size of approximately 30 μm in both phases. Finally, the material was aged at 475 °C for 100 h, resulting in Vickers hardness values of 254 HV in the austenite and 465 HV in the ferrite, respectively. Table 1 gives

* Corresponding author.
E-mail address: alvarez@ifir-conicet.gov.ar (I. Alvarez-Armas).

0142-1123/$ - see front matter © 2012 Elsevier Ltd. All rights reserved.
doi:10.1016/j.ijfatigue.2012.01.010

the tensile properties of the material in the annealed and aged conditions:

Cylindrical shallow-notched specimens for low-cycle fatigue (LCF), Fig. 1a and high-cycle fatigue (HCF), Fig. 1b were manufactured. These geometries ensure that cracks initiate in a limited, approximately flat area within the gauge length. Because the EBSD analysis requires a smooth and defect-free specimen surface, the specimens were ground and electropolished in an electrolyte consisting of 8% perchloric acid, 70% ethanol, 10% diethylene glycol monobutyl ether, and 12% distilled water. The flat part of the notch for LCF was systematically explored during the test using a high resolution CCD camera and the images were stored to record the initiation, growth and propagation of the microcracks. For HCF, the test area of the shallow notch was studied by direct observation in real time using a long-distance QUESTAR optical microscope coupled to a digital camera.

Push–pull LCF tests were performed at room temperature on an electromechanical testing machine. The tests were carried out under plastic-strain control with a fully reversed triangular wave at a constant total strain range of 0.3% and a total strain rate of $2 \times 10^{-3}\ s^{-1}$. In order to record the surface damage, the test was stopped (at 80% of σ_{Max}) periodically. Push–pull HCF tests were carried out in a servo-hydraulic testing system under stress control, $\sigma = 400$ MPa, stress ratio $R = -1$ and $f = 10$ Hz. A 10% decrease in the saturation stress was adopted as the rupture criterion. In the following, the microcrack initiation and propagation behavior was taken as a pattern when it was observed in several grains in the gauge notched area. The tests were repeated in the same conditions to confirm the results.

In order to visualize the microcracks, scanning electron microscopy (SEM) was used in secondary and backscattered electron contrast modes. The EBSD technique was used to determine the distribution of the austenite and ferrite phases and their crystallographic orientations. Internal dislocation structures were studied by transmission electron microscopy (TEM) operated at 100 kV. The thin foils were taken from slices cut at different depths, parallel to the specimen axis, from the shallow-notched area of the specimen on the side opposite the dominant crack. The foils were prepared using a double jet and a solution of 10% perchloric acid and ethanol. Special care was taken to mark the direction of the axial axis of the specimen so that the orientation of each grain relative to the loading direction could be determined. Bright field imaging conditions were adopted and the diffraction patterns were used to determine the grain orientation and main crystallographic directions.

3. Results

Fig. 2 shows the surface damage in the notched area after LCF conducted to rupture.

The combination of the images taken by the CCD camera and the crystallographic analysis by EBSD show that microcracks initiate in the ferrite either on slip planes with the highest SF or at the α/α grain boundary. The cracks then propagate along slip planes also with the highest SF in the neighboring grain (either ferrite or austenite).

In order to analytically characterize the microcrack initiation and propagation, a grain structure map obtained by EBDS was

Table 1
Tensile properties of the duplex stainless steel in the annealed and aged conditions.

	$\sigma_{0.2\%}$ (MPa)	σ_{UTS} (MPa)	E_f (%)
Annealed	525	767	60
Aged	675	978	56

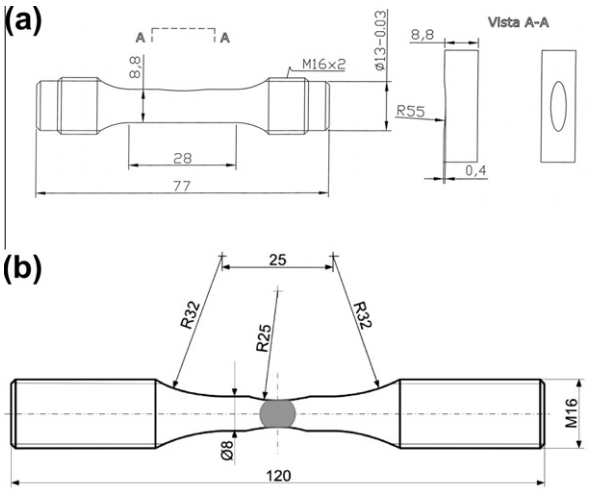

Fig. 1. Geometries of the shallow-notched specimens used for: (a) LCF and (b) HCF (dimensions in mm).

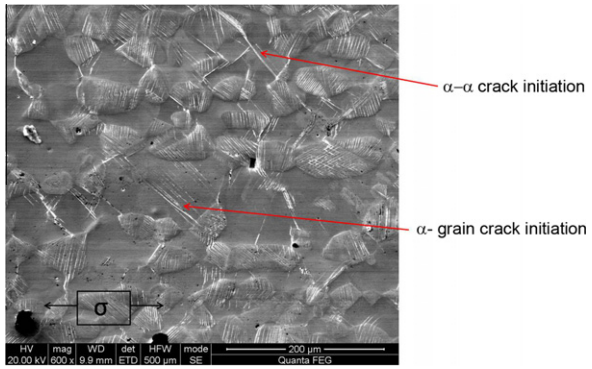

Fig. 2. SEM micrograph showing the surface damage after low cycle fatigue.

overlapped with an image of the fatigue damage recorded by the CCD camera at rupture. This is shown in Fig. 3. In addition, the traces of the activated slip planes and the corresponding SF are indicated. In all the cases, the planes with the highest SF were activated in both phases. The microcrack initiates in the α/α grain boundary (circled area, grains 2–3). First, in the upper part, it remains arrested at the α/γ phase boundary (grains 1–2) whereas it propagates along the lower α grain (grain 4) up to the second α/γ interphase grains 4–5). There, it remains arrested during several cycles and finally, both microcrack tips propagate into the upper (grain 1) and lower (grain 5) austenite grains, respectively.

The inset diagram shows the microcrack growth behavior versus the number of cycles. As reported [11], the microcracks propagate rapidly in the ferritic grains, decelerate or remain stable at the phase boundary and accelerate again, but with a lower rate, having entered the austenitic grain. It is worth mentioning that in the low-cycle fatigue regime, a microstructural crack follows the planes most favorable to slip, i.e. the slip planes with the highest SF.

During HCF, the first slip markings appear in the austenitic phase and to a lesser degree in the ferritic grains. As cycling proceeds, slip lines in the austenitic phase intensify and some propagate into the neighboring ferritic grains or remain arrested at grain boundaries. The slip lines that appear in the ferritic phase propagate into the neighboring ferritic grains or remain arrested at the α–γ phase boundary. Concerning microcrack behavior, three different situations have been observed: (i) initiation at the α–α boundary; (ii) initiation at the α–γ boundary and propagation